JAASP http://www.aaspjournal.org
Journal of Asian Association of Schools of Pharmacy 2022; 11: 6–14

Research Paper

Molecular modelling studies of some furo[2,3-*d*]pyrimidines and pyrrolo[2,3-*d*]pyrimidines as multiple receptor tyrosine kinase inhibitors

Faridah Olubunmi Shuaib[1,*], Malina Jasamai[2] and Kabir Abdu[1]

[1]*Department of Pure and Industrial Chemistry, Bayero University Kano, Kano State, Nigeria*
[2]*Centre for Drug & Herbal Development, Faculty of Pharmacy, Universiti Kebangsaan Malaysia, Kuala Lumpur, Malaysia*

Received August 15, 2022
Revised September 30, 2022
Accepted October 17, 2022

* Corresponding author
Department of Pure and Industrial Chemistry,
Bayero University Kano, Kano, P.M.B. 3011
Kano State, Nigeria
E-mail: bunmmysoul86@gmail.com

ABSTRACT

Tyrosine kinases (TKs) have been implicated in causing tumour growth, angiogenesis and metastasis. Multiple receptor tyrosine kinase (RTK) inhibitors in clinical use have been reported to have adverse effects on hair and skin, hence this makes it impetus to discover new anticancer agents with milder side effects. Furopyrimidines and pyrrolopyrimidines have been reported to exhibit diverse pharmacological properties including TK inhibition. In this study, molecular modelling studies and *in silico* evaluation of pharmacokinetics as well as physicochemical properties were conducted on the furopyrimidines and pyrrolopyrimidines using PyRx-virtual screening tool, Molinspiration and DataWarrior software respectively. The docked compounds exhibited good binding affinity energies and anchored well inside the binding pockets of all the TK receptors used in our study. The predicted pharmacokinetic and physicochemical properties of the compounds showed that they violated one Lipinski's rule of five each and displayed no toxicity potential (mutagenic and tumorigenic), hence this suggests they could pose as potential tyrosine kinases inhibitors candidates with milder side effects.

Key words: tyrosine kinase inhibitors, furo-pyrimidines, pyrrolo-pyrimidines, molecular modelling

1. Introduction

The discovery of protein kinase (PK) inhibitors has tremendously led to a breakthrough in cancer therapy. PKs belong to the class of enzymes that catalyses the phosphorylation of proteins (Ghione et al., 2020). PKs phosphorylate proteins by transferring phosphate group from adenosine triphosphate (ATP) and covalently attaching it to amino acid bearing free hydroxyl (OH) moiety (Marwa et al., 2016). PKs serve a double function; as surface transmembrane receptors as well as enzymes possessing kinase activity. Structurally, kinase receptor is made up of multi-domain extracellular receptor that primarily carries ligand specificity that recognizes an external messenger (growth hormones and growth factors). Furthermore, kinase receptor consists of a single transmembrane hydrophobic helix accompanied by cytoplasmic portion containing kinase domain, which is activated upon binding with receptor-specific ligands causing dimerization of receptor and consequently stimulating cellular processes such as signal transduction, cell proliferation, differentiation, survival, migration and apoptosis (Ansari et al., 2009; Cicenas et al., 2018; Du and Lovly, 2018; Ghione et al., 2020; Paul and Mukhopadhyay, 2004; Pottier et al., 2020).

PKs are further divided into tyrosine and serine-threonine kinases based on substrate specificity (Shchemelinin et al., 2006). Protein tyrosine kinases which are enzymes that provide central switch mechanism in cellular signal transduction are classified into receptor tyrosine kinase (RTK) [epidermal growth factor receptor (EGFR), vascular endothelial growth factor receptor (VEGFR), platelet-derived growth factor receptor (PDGFR), fibroblast growth factor receptor (FGFR), c-mesenchymal epithelia transition factor (C-MET) and insulin receptor (IR)] and non-receptor tyrosine kinase (NRTK) [proto-oncogene (SRC), Abelson (ABL), focal adhesion kinase (FAK) and Janus kinase]. C-Met, VEGF and EGF families have been reported to take part in cellular processes and implicated in causing tumour growth,

angiogenesis and metastasis. VEGF, FGF, PDGF, angiopoietin-2 (Ang-2), hepatocyte growth factor and insulin-like growth factor (ICF) are considered as pro-angiogenic growth factors as they are expressed in cancer cell (Abou El Ella et al., 2008).

On the other hand, fused pyrimidines such as furopyrimidines and pyrrolopyrimidines have been reported to exhibit diverse pharmacological properties such as antitumor, anticancer, antiviral, antimicrobial, antifolate as well as protein kinase inhibitors (Sroor et al., 2019).

In view of the aforementioned study on fused pyrimidines, structure activity relationship of marketed protein tyrosine kinase inhibitors and in continuation of our previous work on screening the pharmacological properties of fused pyrimidines, this study described the *in-silico* evaluation of some furo[2,3-*d*]pyrimidine and pyrrolo[2,3-*d*]pyrimidine derivatives (Figure 1) as potential multiple RTKs inhibitors which can be developed as anticancer agents.

2. Materials and Methods

The *in-silico* studies were performed using Avita workstation running on advance micro devices (AMD) ryzen 5, 8 GB random access memory (RAM), 512 GB hard disk. PyRx-virtual screening tool was engaged in carrying out the docking study.

2.1. Molecular modelling study

The molecular modelling study was performed using PyRx-Virtual Screening Tool (Trott and Olson, 2010). ChemDraw professional 15.0 was employed in sketching the 2-dimentional (2D) structure of the ligands. The sketched ligands were copied to Chem3D and saved in .pdb format. Autodock "make ligand" tool was used to prepare the ligands. Crystal structures of the targets [EGFR; PDB ID: 5ZTO (Zhu and Yun, 2018), VEGFR-2; PDB ID: 3VHE (Oguro et al., 2011) and PDGFRA; PDB ID: 6JOL (Liang et al., 2016)] were all downloaded from (www.rcsb.org). These protein crystal structures were prepared using Autodock make macromolecule tool. The tool optimized hydrogen bonds removed all bound water molecules, ligands, and cofactors from the protein in .pdb format and saved the prepared proteins in .pdbqt format. The final configuration grid.txt was set at 58, 35 and 55 for x, y and z axes respectively. The validation of the docking method was carried out using root mean square deviation (RMSD). This method gives an insight on the ability of the molecular modelling to reproduce an experimental ligand-binding mode. The co-crystallised ligands were re-docked back into the binding site of the various proteins and all the RMSDs derived falls within the acceptable range (RMSD ≤ 2), hence the docking protocol was adopted in this study. The docking results were visualised and analysed using BIOVIA discovery studio 2021

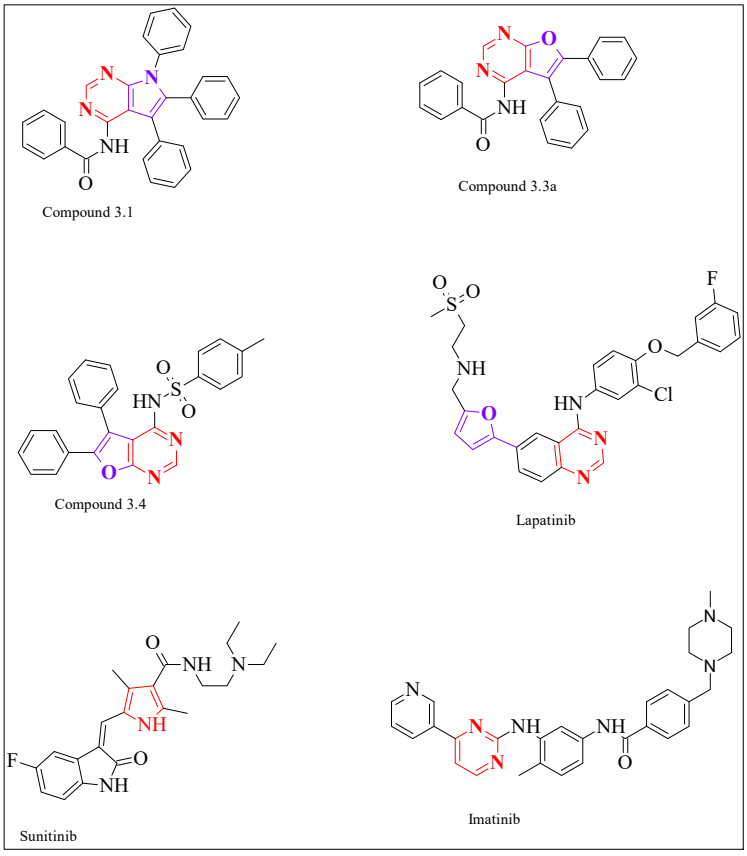

Figure 1. Structures of the docked furo[2,3-*d*]pyrimidine and pyrrolo[2,3-*d*]pyrimidine derivatives and some marketed receptor tyrosine kinase inhibitors.

client and PYMOL. The ligand–enzyme interactions were described by binding affinity.

2.2. Prediction of in silico ADME (absorption, distribution, metabolism and excretion) properties of the fused pyrimidines

Molinspiration, a free online software (http://www.molinspiration.com/cgi-bin/properties) was employed in predicting the molecular properties and bioactivity scores for all the synthesised compounds. The bioactivity scores for G-protein-coupled receptors (GPCR), ion channel modulators, kinase inhibitors, nuclear receptors, protease and enzyme inhibitors were all predicted. Molecular parameters such as; molecular weight (MW), partition coefficient (*mi*LogP) (lipophilicity), number of rotatable bonds (*n*-rotb), number of atom (*n*-atoms), topological polar surface area (TPSA), number of hydrogen bond acceptors (*n*-ON) and number of hydrogen bond donors (*n*-OHNH) and violation of Lipinski's rule of five were all predicted in order to evaluate the drug-likeness of the furo[2,3-*d*]pyrimidine and pyrrolo[2,3-*d*]pyrimidine derivatives. The absorption percentage (%Ab) for each ligand was calculated using method described by Zhao et al., 2002. [% Ab = 109 – (0.345×TPSA)]. DataWarrior developed by Osiris property explorer (http://www.organic-chemistry.org/prog/peo) was employed in predicting the drug-likeness, solubility, toxicity (mutagenic, tumorigenic) potential and possible irritant effect of furo[2,3-*d*]pyrimidine and pyrrolo[2,3-*d*]pyrimidine derivatives.

3. Results and Discussion

3.1. Molecular docking of furo[2,3-d]pyrimidine and pyrrolo[2,3-d]pyrimidine derivatives as potential EGFR inhibitors

Binding affinity energy reflects the strength of interaction and affinity between ligand and protein. Among the docked compounds, compound **3.4** (*N*-(5,6-diphenylfuro[2,3-*d*]pyrimidin-4-yl)-4-methylbenzenesulfonamide) was found to have the best affinity energy (–9.4 kcal/mol) and anchored well inside the binding site of EGFR. Lapatinib, compounds **3.1** (*N*-5,6,7-triphenyl-pyrrolo[2,3-*d*]pyrimidin-4-yl) benzamide), **3.3a** (*N*-(5,6-diphenylfuro[2,3-*d*] pyrimidin-4-yl)benzamide, imatinib and sunitinib bound with minimum binding affinity energies of –8.6, –8.5, –8.1, –7.4 and –7.1 kcal/mol respectively as illustrated in Figure 2. Furthermore, the binding interaction of lapatinib (marketed EGFR inhibitor) with EGFR revealed the formation of three significant hydrogen bond interactions with amino acid residues Glu1015 (2.52 Å) and Val1010 (2.58 Å) through its pyrimidine and NH moieties and the other hydrogen bond with Thr993 (2.12 Å) through its sulfoxide moiety. Similarly, lapatinib displayed van der Waals interactions with Pro741, Phe795 and Ser991. The other interactions were π-anion with Glu1015 through its furan moiety, π-sigma with Pro794, π-π T-shaped with Phe997 (5.11 Å) and π-alkyl with Pro992 (5.23 Å). On the other hand, compound **3.4** formed two hydrogen bond interactions with amino acid residues Lys728 and Asp1012 through its sulfoxide and pyrimidine moieties. Sulfoxide moiety of compound **3.4** mimicked that of lapatinib by forming significant hydrogen bond with crucial amino acid residue found in EGFR active site, this could possibly justify its good binding affinity towards EGFR. The other interactions were π-sigma with Val1010 through its furan moiety, π-π stacked with Phe997, alkyl with Phe795, Pro992 and π-alkyl with Pro741, Pro794. In a similar way compound **3.1** carbonyl moiety formed significant hydrogen bond interaction with amino acid residue Lys728 (2.48 and 2.84 Å). Other interactions formed by compound **3.1** were π-cation with Lys728, π-sulfur with Met1007, π-π T-shaped with Phe997 and π-alkyl with Leu730, Pro741, Pro794, Val1010. Compound **3.3a** demonstrated a good binding affinity towards EGFR by forming significant hydrogen bond interaction with Asp1012 (1.9 and 2.88 Å), π-π Stacked with Phe977 through its furan moiety, and π-alkyl with Pro741,

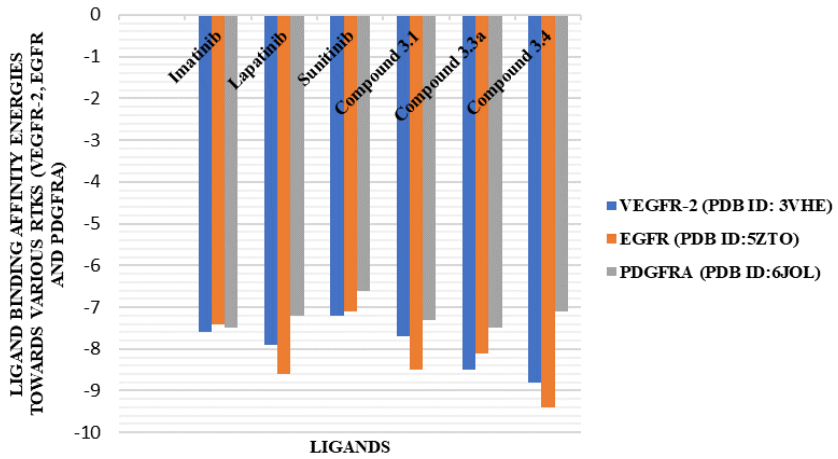

Figure 2. Ligand binding affinity energies between docked compounds and crystal structures of VEGFR, EGFR, and PDGFRA.

Pro794 and Val1010 residues as illustrated in Figures 3 & 4. Presumably, formation of π-π stacked/ π T-shaped interaction with amino acid residue Phe997 and presence of amide linkage as well as pyrimidine moieties are key requirements for effective inhibition of EGFR.

3.2. Molecular docking of furo[2,3-d]pyrimidine and pyrrolo[2,3-d]pyrimidine derivatives as potential VEGFR2 inhibitors

The binding affinity energies between the fused pyrimidines and VEGFR2 were obtained from analysis of molecular docking and compared with sunitinib, a VEGFR2 inhibitor. Compound **3.4** bound to the target protein VEGFR2 with the least binding affinity energy of –8.8 kcal/mol and the best in term of docking score. Compounds **3.3a**, **3.1** and Sunitinib bound with minimum binding energies of –8.5, –7.7 and –7.2 kcal/mol respectively as illustrated in Figure 2. Analysis of the binding mode of sunitinib, revealed formation of van der Waals interactions with the amino acid residues Arg842, Asn923, Ser925, Thr926, Arg929, Arg1032, Ala1050, Asp1052, Asp1056, Pro1057, Asp1058, Trp1071, Glu1097, Ser1104, Pro1105. In addition, sunitinib formed carbon-hydrogen bond interaction with Gly1102, π-donor hydrogen with Phe1047 and π-cation interaction with Arg1051 through its pyrrole moiety. The other interactions were π-π T-shaped with Phe1047, alkyl and π-alkyl with Arg1051. Similarly, binding mode analysis of compound **3.4** showed that it demonstrated very good interactions in the VEGFR2 binding site by forming significant hydrogen bond interaction with amino acid residue Arg1027 (2.76 Å). Compound **3.4** formed van der Waals with Lys868, Glu885, π-cation as well as π-anion with Asp1046 and Asp814 through its furan and phenyl moiety respectively. Other molecular interactions include carbon hydrogen bond with Gly1048, π-donor hydrogen bond with Leu1049, alkyl with Leu882, Leu1049 and π-alkyl with Ala881. Compound **3.3a** formed π-anion interaction with Asp1046 through its furan moiety, weak π-sulfur interaction with Cys817 (5.22 Å) as well as π-alkyl interactions with amino acid residues Ala881 (4.94 Å), Ile888 (4.87 Å) and Ile1053 (4.42 Å). Pyrrole moiety of compound **3.1** formed π-anion interaction with Asp1056 and a strong hydrogen bond interaction with Arg842 (2.46 Å) through its pyrimidine moiety. Other interactions were carbon hydrogen bond with Ala50, π-donor hydrogen bond with Phe1047 and π-alkyl with Arg1051 (4.84 Å) through its pyrrole group (Figures 5 & 6). Furthermore, formation of π-cation/anion with crucial amino acid residues through pyrrole/furan moiety of the docked compounds is presumably paramount for effective inhibition of VEGFR2.

3.3. Molecular docking of furo[2,3-d]pyrimidine and pyrrolo[2,3-d]pyrimidine derivatives as potential PDGFRA inhibitors

Binding interactions of furopyrimidine and pyrrolopyrimidine derivatives were compared with imatinib, the co-crystallised ligand of PDGFRA. Compound **3.3a** demonstrated the least binding energy of –7.5 kcal/mol, followed by compound **3.1** and **3.4** with minimum binding energies of –7.3 and 7.1 kcal/mol respectively. Compound **3.3a** demonstrated equal binding affinity with imatinib towards PDGFRA as illustrated in Figure 2. In addition, analysing the binding modes of imatinib revealed the formation of significant conventional hydrogen bond interaction between amide carbonyl group of imatinib and NH of Asn656 residue (2.44 Å) and carbon hydrogen bond between pyridine moiety of imatinib and amino acid residue Glu951. Similarly, compound **3.3a** formed significant hydrogen bond with Gly838 residue (2.96 Å) through its amide carbonyl group as well van der Waals interactions with amino acid residues Ser643, Glu644, Leu839, Tyr849, Phe856, Leu85 and Pi-anion interactions with Asp818, Asp818. Benzamido and phenyl moieties of compound **3.3a** also formed weak π-alkyl interactions with amino acid residues Ala640 (4.75 Å), Ile843 (5.29 Å) and Pro858 (5.48 Å). Compound **3.1** with amide linkage also demonstrated good binding affinity towards PDGFR by forming significant hydrogen bond interaction with Gly829 (2.89 Å) through its pyrimidine moiety, van der Waals interactions with Asn656, Ser797, Gln801, Arg804, Glu951, Gly956, π-sigma interaction with Leu954 through its phenyl moieties with bond length of 3.62 Å. It also formed π-π T-shaped and π-alkyl interactions with amino acid residues Tyr800 (4.87 and 5.06 Å) and Leu793 (5.23 and 5.50 Å) respectively through its phenyl moieties. Furthermore compound **3.4** also demonstrated very promising binding affinity by forming significant hydrogen bond interactions with amino acid residues Asp794 (2.36 and 2.70 Å), Gln801 (2.68 Å), and Lys830 (2.11 Å) through its furopyrimidine scaffold, carbon hydrogen bond as well as π-donor hydrogen bond interactions with Ser797 (3.67 Å) residue. Alkyl and π-alkyl interactions with Leu954 (4.26 and 4.33 Å) and Ile831 (5.433 Å) respectively as shown in Figures 7 & 8.

3.4. Prediction of pharmacokinetic properties, bioactivity profile and toxicity potential of furo[2,3-d]pyrimidine and pyrrolo[2,3-d]pyrimidine derivatives

When designing drug, human oral bioavailability is an important parameter to be taken into consideration. Human oral bioavailability of an active molecule is determined through its absorption, distribution, metabolism, excretion and toxicity (ADME-T), (Elsisi et al., 2021). To predict human oral bioavailability of the compounds, Lipinski rule of five which is widely used in drug design and discovery was employed. Molecules violating more than one Lipinski rule will likely exhibit poor permeation and bioavailability. All the fused pyrimidine derivatives compound (**3.1**, **3.3a** and **3.4**) violated one Lipinski's rule of five where *CLogP* values for all the docked compounds were found to be slightly above

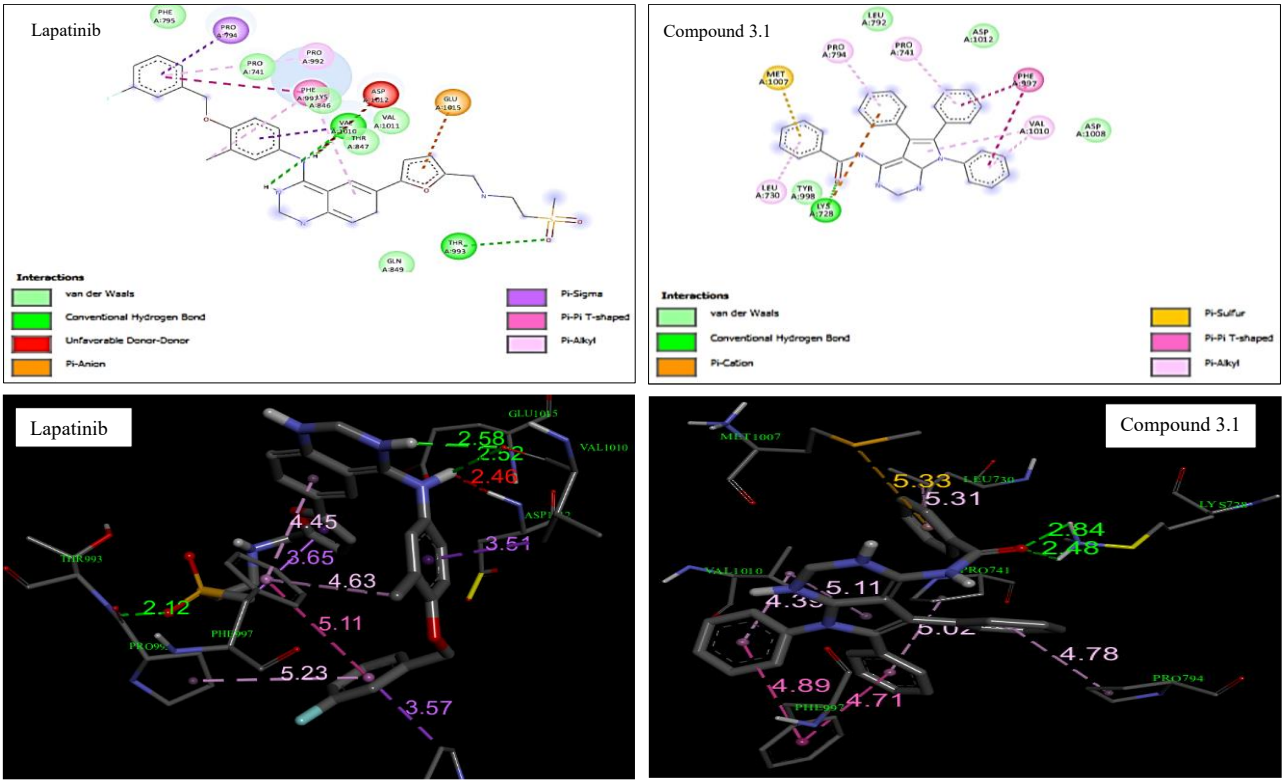

Figure 3. Binding interaction (2D & 3D) of lapatinib and compound 3.1 within the binding site of EGFR (PDB ID: 5ZTO) revealing various interactions with amino acid residues.

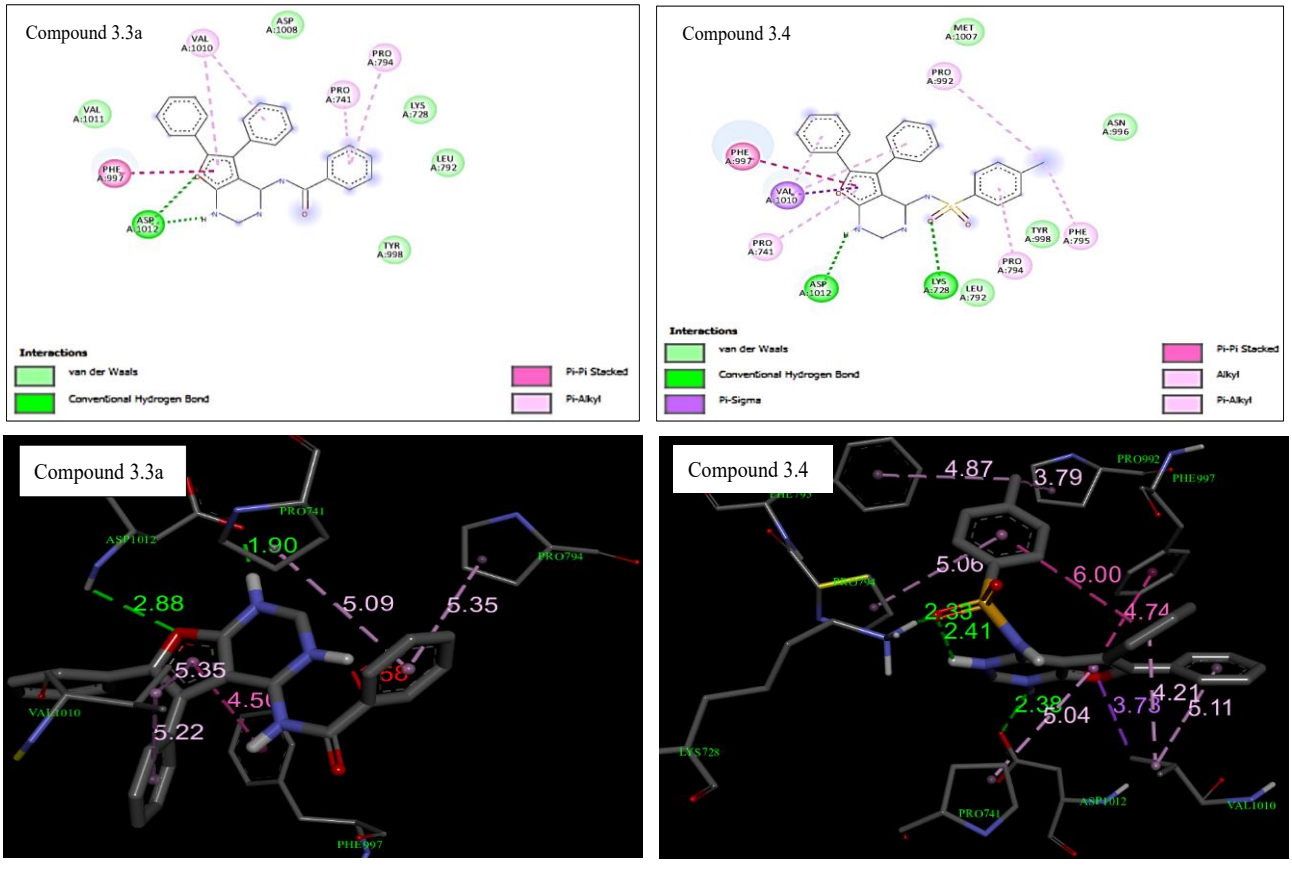

Figure 4. Binding interaction (2D & 3D) of compound 3.3a and 3.4 within the binding site of EGFR (PDB ID: 5ZTO) revealing various interactions with amino acid residues.

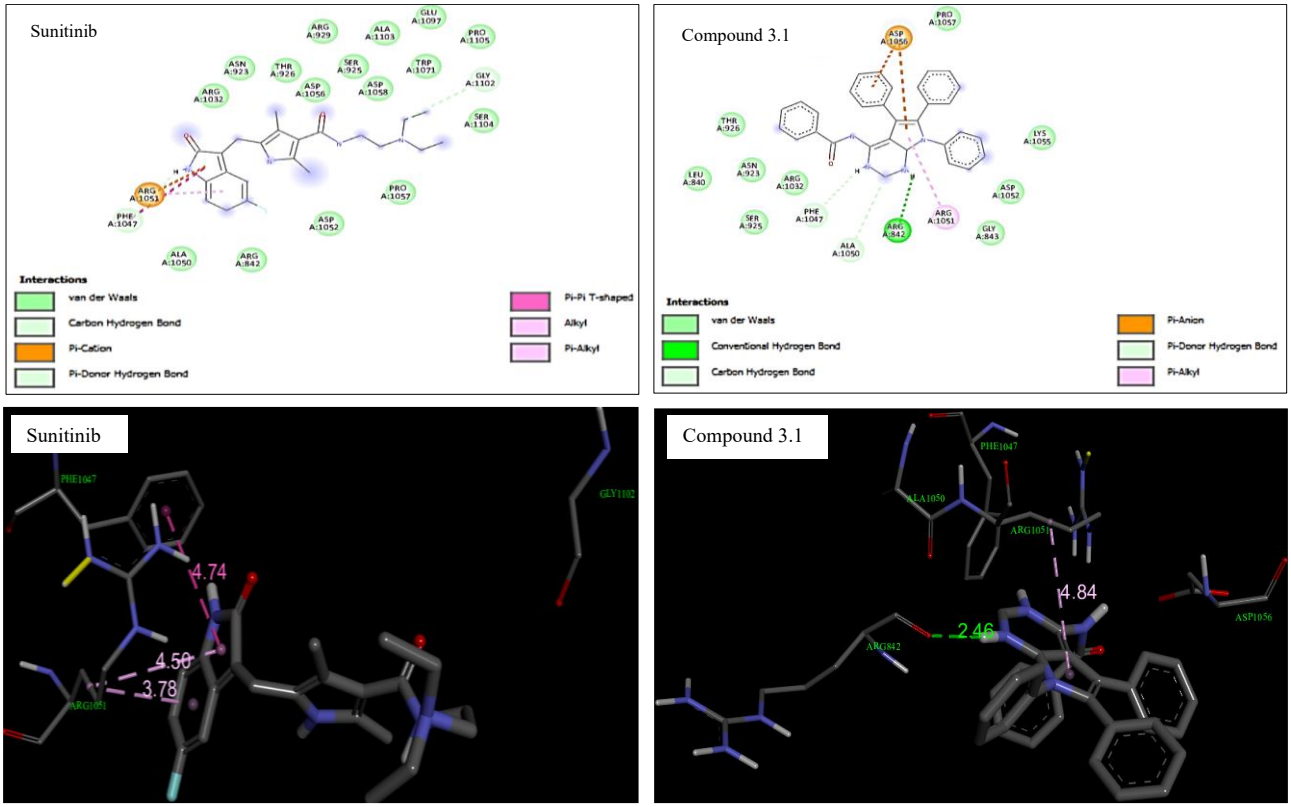

Figure 5. Binding interaction (2D & 3D) of sunitinib and compound 3.1 within the binding site of VEGFR2 (PDB ID: 3VHE) revealing various interactions with amino acid residues.

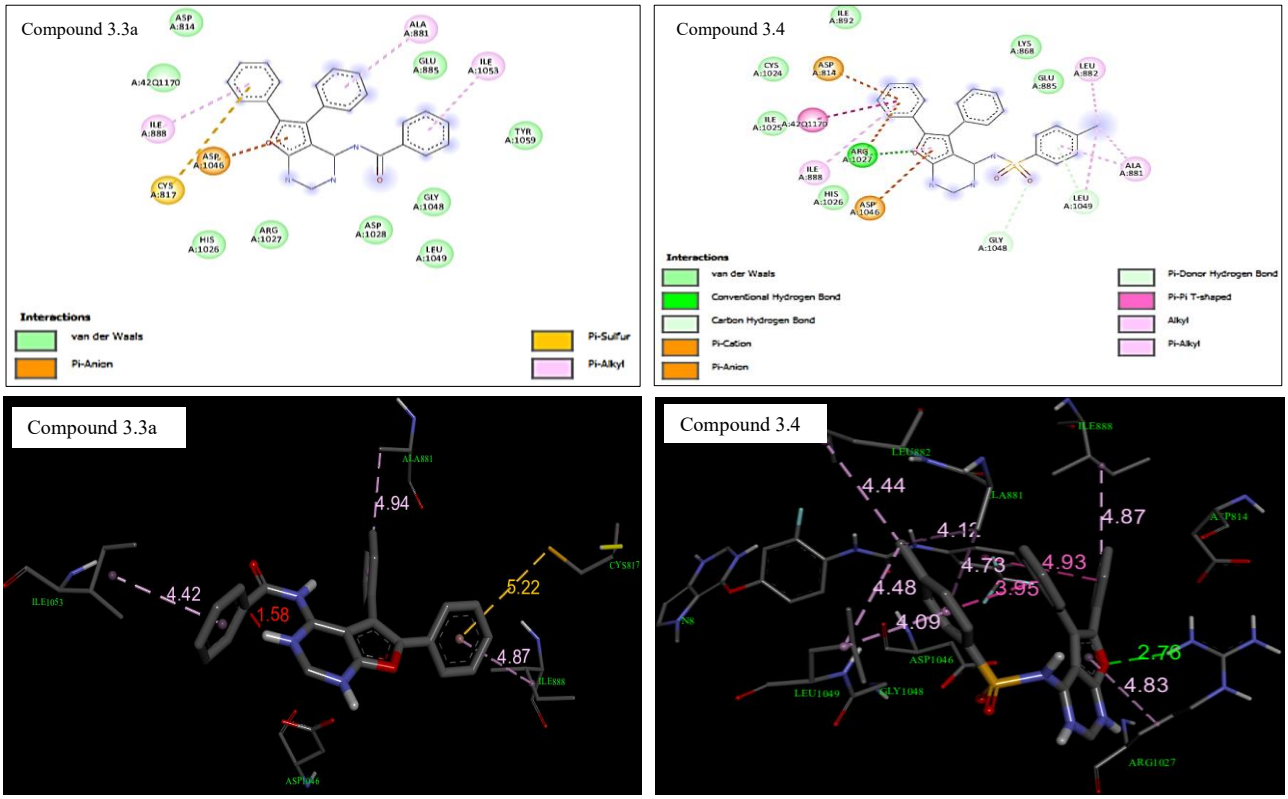

Figure 6. Binding interaction (2D & 3D) of compound 3.3a and 3.4 within the binding site of VEGFR2 (PDB ID: 3VHE) revealing various interactions with amino acid residues.

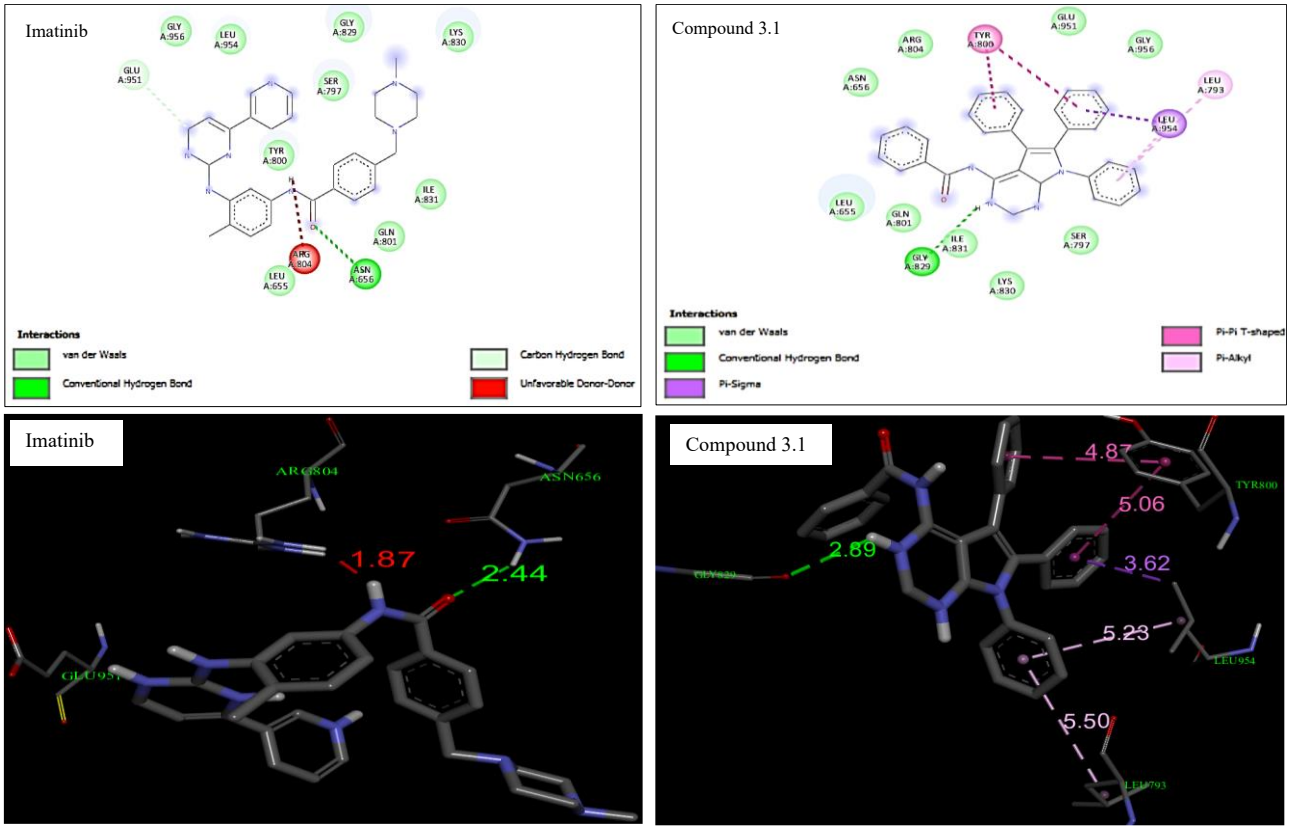

Figure 7. Binding interaction (2D & 3D) of imatinib and compound 3.1 within the binding site of PDGFRA (PDB ID: 6JOL) revealing various interactions with amino acid residues.

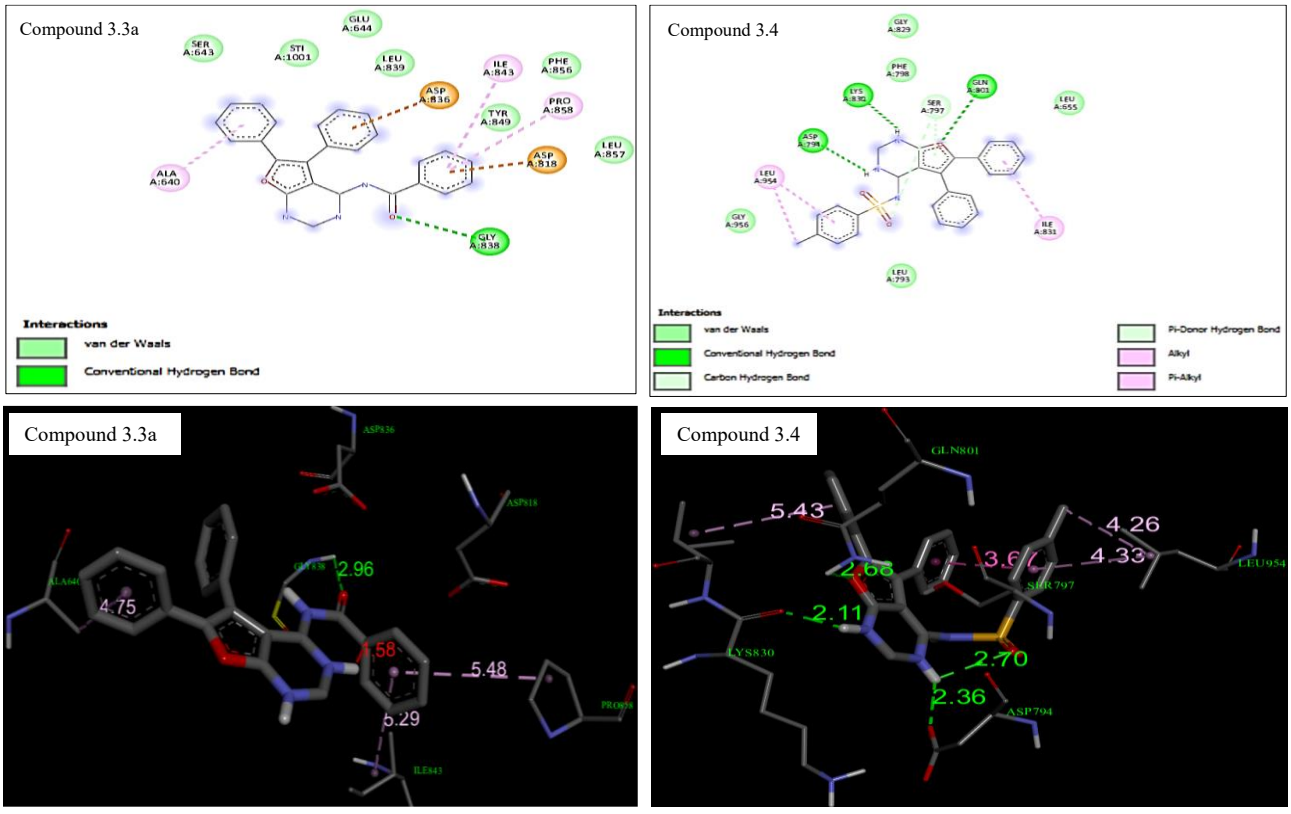

Figure 8. Binding interaction (2D & 3D) of compound 3.3a and 3.4 within the binding site of PDGFRA (PDB ID: 6JOL) revealing various interactions with amino acid residues.

Table 1. Evaluation of physicochemical and pharmacokinetic properties of the reference drugs and synthesised fused pyrimidine derivatives in accordance with Molinspiration cheminformatic software.

Compound	MW[a]	*miLogP*[b]	$_n$ON[c]	$_n$OHNH[d]	$_n$Lipinstic violations[e]	$_n$rotb[f]	$_n$Atoms[g]	TPSA[h] (Å)	%ABS[i]
3.1	466.54	6.30	5	1	1	5	36	59.81	88.4
3.3a	391.43	5.31	5	1	1	4	30	68.02	85.5
3.4	441.51	5.63	6	1	1	5	32	85.09	79.6
Imatinib	493.62	3.89	8	2	0	7	37	86.28	83.3
Lapatinib	581.07	6.16	8	2	2	11	40	106.35	70.9
Sunitinib	398.48	1.95	6	3	0	7	29	80.99	77.6

[a]Molecular weight (MW < 500g/mol); [b]Logarithm of partition coefficient between n-octanol and water (miLogP ≤ 5); [c]Number of hydrogen bond acceptors (*n*-ON < 10); [d]Number of hydrogen bond donors (*n*-OHNH <5); [e]Number Lipinski's rule violated (*n*-Lipinski's rule violation); [f]Number of rotatable bond (*n*-rotb < 10); [g]Number of atoms (*n*-atoms); [h]Topological polar surface area (TPSA < 160Å); [i]Percentage human absorption (%ABS scale 0–100%, >80% high, < 24 poor).

Table 2. Bioactivity score for the synthesised fused pyrimidine derivatives in accordance with Molinspiration cheminformatic software.

Compound	GPCR Ligand	Ion channel modulator	Kinase inhibitor	Nuclear receptor ligand	Protease inhibitor	Enzyme inhibitor
3.1	–0.04	–0.27	0.37	–0.35	–0.29	–0.02
3.3a	–0.17	–0.41	0.55	–0.58	–0.37	0.05
3.4	–0.20	–0.53	0.30	–0.51	–0.36	0.01
Imatinib	0.10	–0.09	0.59	–0.40	–0.08	0.07
Lapatinib	–0.04	–0.52	0.36	–0.35	–0.21	–0.08
Sunitinib	–0.16	–0.62	0.51	–0.80	–0.51	–0.23

Bioactivity score scale; > 0.0 = very active, –5–0= moderately active, < –5 = inactive.

the acceptable range (*LogP* > 5). *LogP* stand for molecular hydrophobicity or lipophilicity of a molecule and these compounds having *LogP* values slightly greater than the acceptable range may indicate poor permeability across the cell membrane. The molecular weight of all the docked compounds falls within the acceptable range (MW ≤500 g/mol), thus the docked molecules are predicted to be readily transported, diffused, and absorbed compared to large molecules. The number of hydrogen bond acceptors, donors and rotatable bonds for all the compounds is in accordance with Lipinski's rule. Topological polar surface area (TPSA) predicted for all the furo[2,3-*d*]pyrimidine and pyrrolo[2,3-*d*]pyrimidine derivatives ranging from 59.81 to 85.09Å falls within acceptable range ≤160 Å, thus indicating potential good oral bioavailability as shown in Table 1.

Bioactivity score is an important parameter that gives an insight on the molecular activity or possibility of a compound to be a drug candidate. The bioactivity scores for all the docked compounds were predicted based on the following drug targets; G protein-coupled receptors (GPCR) (50% of marketed drugs targets GPCR (Trazkowski et al., 2012)), ion channel modulator, kinase inhibitor (target for most anticancer drugs), nuclear receptor, protease inhibitor (target for some antiviral drugs) and enzyme inhibitor (e.g., some antibacterial drugs exert their effect by inhibiting enzymes such as DNA gyrase and dihydrofolate reductase). Compound exhibiting bioactivity score of greater than 0.0 and –0.5 to 0.0 indicates good and moderate biological activities respectively. However, bioactivity score of less than –0.5 may suggest inactivity. All the docked fused pyrimidines demonstrated a good to moderate kinase and enzyme inhibitory activities, this suggests them of having potential anticancer and antibacterial activity respectively. In addition, they all exhibited good to moderate G-protein couple protein (GPCR) ligand and moderate protease inhibitory activity, while compound **3.1** posed as moderate ion channel modulator and nuclear receptor ligand as illustrated in Table 2. GPCR are involved in wide range of signalling pathways related to many pathological processes such as cancer, inflammatory, mental and metabolic disorders, viral infections, cardiovascular and endocrine disorders, thus making them target for pharmaceutical (Trazkowski et al., 2012). On the other hand, ion channels in the presence of some ligands (drugs, neurotransmitters, plant, and animal toxins) controls the influx of ions into the membrane which concomitantly leads to cellular processes. This process can be therapeutic (antiarrhythmics and antiepileptics) (Tasneem et al., 2005). Similarly, nuclear receptors regulate gene expression in the presence of ligands, thus this made them an important target for pharmaceuticals (Olefsky, 2001).

Table 3: Evaluation of drug-likeness, toxicity potential (mutagenic & tumorigenic) and irritant effect of compounds 3.1, 3.3a and 3.4 in accordance with DataWarrior (Osiris property explorer).

Compound	Drug-likeness	Mutagenic	Tumorigenic	Irritant effect
3.1	2.24	none	none	none
3.3a	1.13	none	none	none
3.4	–5.49	none	none	none
Imatinib	8.6128	none	none	none
Lapatinib	–4.2297	none	none	none
Sunitinib	8.335	none	none	none

The toxicity potential, irritant effect, and drug-likeness of all the docked compounds were also investigated. Compounds **3.1** and **3.3a** have a very promising drug-likeness scores while all the compounds (**3.1**, **3.3a** and **3.4**) have low probability of having toxicity (mutagenic & tumorigenic) potential and irritant effect as shown below in Table 3.

4. Conclusion

In this study, the molecular docking studies of series of furo[2,3-*d*]pyrimidine and pyrrolo[2,3-*d*]pyrimidine derivatives were reported as potential multi-RTKs inhibitors, thus as potential anticancer agents. All the compounds especially compound **3.4** showed very good binding affinities and anchored well inside the binding pockets of all the tyrosine kinase receptors used. The predicted pharmacokinetic properties and toxicity potentials revealed that all the compounds **3.1**, **3.3a** and **3.4** violated one Lipinski's rule of five each as well as exhibited very good percentage human oral absorption (79.6–88.4%) and no toxicity potential (mutagenic, tumorigenic and irritant) effects.

However, our next line of investigation is to carry out modification of pharmacophoric features of compound **3.1**, **3.3a** and **3.4** in such a way that their good binding affinities towards protein tyrosine kinase receptors would be retain and as well satisfying all the Lipinski's rules of five, hence this could lead to discovery of alternative anticancer drugs with tolerable side effects.

Conflict of Interest

The authors declare no conflict of interest.

References

Abou El Ella DA, Ghorab MM, Noaman E, Heiba HI and Khalil AI. Molecular modelling study and synthesis of novel pyrrolo[2,3-*d*]pyrimidines and pyrrolotriazolopyrimidines of expected antitumor and radioprotective activities. Bioorg Med Chem. 2008; 16(5): 2391-2402.

Ansari J, Palmer DH, Rea DW and Hussain SA. Role of tyrosine kinase inhibitors in lung cancer. Anti-Cancer Agents Med Chem. 2009; 9: 569-575.

Calculation of molecular physicochemical properties-Molinspiration. Available from: http://www.molinspiration.com/cgi-bin/properties.

Cicenas J, Zalyte E, Bairooch A and Gaudet P. Kinases and cancer. Cancers. 2018; 10: 2-7.

Du Z and Lovly CM. Mechanism of receptor tyrosine kinase activation in cancer. Mol Cancer. 2018;17: 1-13.

Elsisi DM, Ragab A, Elhenawy AA, Farag AA, Ali AM and Ammar YA. Experimental and theoretical investigation for 6-morpholinosulfonylquinoxalin-2(1*H*)-one and its haydrazone derivative: Synthesis, characterisation, tautomerization and antimicrobial evaluation. J Mol Struct. 2021; 1247: 1- 10.

Ghione S, Mabrouk N, Paul C and Bettaieb A. Protein kinase inhibitor-based cancer therapies: Considering the potential of nitric oxide (NO) to improve cancer treatment. Biochem Pharmacol. 2020; 176: 1-11.

Liang L, Yan XE and Yun CH. Crystal structure of PDGFR in complex with imatinib by co-crystallization. [Internet]. 2020 Mar 25 [cited 2022 Feb 10]. Available from: http://www.rcsb.org.

Marwa AA, Serya RAT, Lasheen DS and Abouzid KAM. Furo[2,3-d]pyrimidine based derivatives as kinase inhibitors and anticancer agents. Future J Pharma Sci. 2016; 2: 1-8.

Oguro Y, Miyamoo N, Okada K, Takagi T, Iwata H, Awazu Y, et al. Crystal structure of human VEGFR2 kinase domain with a novel pyrrolopyrimidine inhibitor. Bioorg Med Chem. 2011; 18(20): 7260-7273.

Olefsky JM. Nuclear receptor. J Biol Chem. 2001;276(40): 36863-36864.

Paul MK and Mukhopadhyay AK. Tyrosine kinase-Role and significance in cancer. Int J Med Sci. 2004; 1: 101-115.

Pottier C, Fresnais M, Gilon M, Jerusalem G, Longuespee R and Souni NE. Tyrosine kinase inhibitors in cancer: Breakthrough and challenges of targeted therapy. Cancers. 2020; 12(3): 731.

Shchemelinin I, Šefc L and NeČas E. Protein kinases, Their function and implication in cancer and other diseases. Folia Biol. 2006; 52: 81-101.

Sroor FM, Basyouni WM, Tohamy WM and Abdelhafez TH. Novel pyrrolo[2,3-*d*]pyrimidine derivatives: Design, synthesis structure elucidation and *in vitro* anti-BVDV activity. Tetrahedron. 2019; 75(51): 1-10.

Tasneem A, Lakshminarayan MI, Eric J and Aravind L. Identification of prokaryotic ligand-gated ion channels and their implication for the mechanisms and origin of animal Cys-loop ion. Genome Biol. 2005; 6(1): R4.

Trott O and Olson AJ. Autodock Vina: improving the speed and accuracy of docking with a new scoring function, efficient optimization and multithreading. J Comput Chem. 2010; 31(2): 455-461.

Trzaskowski B, Latek D, Yuan S, Ghoshdastider U, Debinski A and Filipek S. Action of molecular switches in GPCRs-Theoretical and experimental studies. Curr Med Chem. 2012; 19: 1090-1109.

Zhao Y, Abraham MH, Le J, Hersey A, Luscombe CN, Beck G, et al. Rate-limited steps of human oral absorption and QSAR studies. Pharm Res. 2002; 19(10): 1446-1457.

Zhu SJ and Yun CH. Crystal structure of EGFR 696-1022 T790/C79S in complex with D3003. [Internet]. 2019 Jun 12 [cited 2022 Feb 10]. Available from: http://www.rcsb.org.